

One-dimensional discrete aggregation-fragmentation model

N. Zh. Bunzarova ^{†1†2}, N. C. Pesheva ^{†2} and J. G. Brankov ^{†1†2}

^{†1} *Bogoliubov Laboratory of Theoretical Physics,*

Joint Institute for Nuclear Research, 141980 Dubna, Russia and

^{†2} *Institute of Mechanics, Bulgarian Academy of Sciences, 1113 Sofia, Bulgaria*

We study here one-dimensional model of aggregation and fragmentation of clusters of particles obeying the stochastic discrete-time kinetics of the generalized Totally Asymmetric Simple Exclusion Process (gTASEP) on open chains. Isolated particles and the first particle of a cluster of particles hop one site forward with probability p ; when the first particle of a cluster hops, the remaining particles of the same cluster may hop with a modified probability p_m , modelling a special kinematic interaction between neighboring particles, or remain in place with probability $1 - p_m$. The model contains as special cases the TASEP with parallel update ($p_m = 0$) and with sequential backward-ordered update ($p_m = p$). These cases have been exactly solved for the stationary states and their properties thoroughly studied. The limiting case of $p_m = 1$, which corresponds to irreversible aggregation, has been recently studied too. Its phase diagram in the plane of injection (α) and ejection (β) probabilities was found to have a different topology.

Here we focus on the stationary properties of the gTASEP in the generic case of attraction $p < p_m < 1$ when aggregation-fragmentation of clusters occurs. We find that the topology of the phase diagram at $p_m = 1$ changes sharply to the one corresponding to $p_m = p$ as soon as p_m becomes less than 1. Then a maximum current phase appears in the square domain $\alpha_c(p, p_m) \leq \alpha \leq 1$ and $\beta_c(p, p_m) \leq \beta \leq 1$, where $\alpha_c(p, p_m) = \beta_c(p, p_m) \equiv \sigma_c(p, p_m)$ are parameter-dependent injection/ejection critical values. The properties of the phase transitions between the three stationary phases at $p < p_m < 1$ are assessed by computer simulations and random walk theory.

Keywords: non-equilibrium phenomena, one-dimensional processes, generalized TASEP, stationary states, phase transitions

I. INTRODUCTION

Different variants of TASEP model are widely studied currently, since it is believed that this model can be helpful in understanding various types of systems in Nature, such as: kinetics of protein synthesis [1, 2], molecular motors on a single track [3], colloid particles moving in narrow channels [4–6], and vehicles on a single-lane road [7–10], etc. Another motivation for studying TASEP-like models is the aim for a better understanding of the properties of systems in nonequilibrium steady states, nonequilibrium phase transitions and various phenomena with no counterpart in the equilibrium case. In the model under consideration here, the particles obey the dynamics of the generalized Totally Asymmetric Simple Exclusion Process (gTASEP), which essentially is the TASEP with backward-sequential update equipped with two hopping probabilities: p and p_m . The modified hopping probability $p_m > p$ describes a kinematic attraction between neighboring particles which hop during the same integer-time moment. In principle, the model admits the study of aggregation-fragmentation phenomena, fluctuations and finite-size effects in nonequilibrium stationary states induced by the boundary conditions.

We remind the reader that the original TASEP was defined as a continuous-time Markov process (random-sequential update in the Monte Carlo simulations) and was solved exactly with the aid of recurrence relations by Domany et al [11] for special values of the model parameters, and by Schütz and Domany [12] in the general case. A breakthrough in the methods for solving TASEP on open chains marks the matrix-product representation of the steady-state probability distribution, found in [13]. Different versions of this approach, known as the Matrix Product Ansatz (MPA), were used also to obtain exact solutions for the stationary states of TASEP and ASEP under several types of discrete-time stochastic dynamics: sublattice-parallel [14, 15], forward-ordered and backward-ordered sequential [16, 17], and fully parallel (simultaneous updating of all sites) [18], [19]. The above studied cases of TASEP show that the only dynamics that allow clusters to move forward as a whole entity is the backward-ordered one. Then, the probability for translation of a cluster of k particles one site to the right is p^k , while such a cluster is broken into two parts with probability $p - p^k$. Under the generalized TASEP dynamics, the probability for translation of a cluster of k particles one site to the right becomes pp_m^{k-1} , and its fragmentation into two parts happens with probability $p(1 - p_m^{k-1})$.

We note that the above generalized backward-ordered dynamics was suggested as exactly solvable one by Wölki [20], and studied on a ring in [21–23]. The limit case of $p_m = 1$ corresponds to irreversible aggregation, or jam formation in the case of vehicles, suggested and studied by Bunzarova and Pesheva [24] and further elaborated in [25, 26]. Here, we focus on the stationary properties of gTASEP when $p < p_m < 1$, describing the generic case of attraction between particles hopping stochastically and unidirectionally in discrete time along finite one-dimensional chains with given boundary conditions at the ends.

II. THE MODEL AND SOME KNOWN RESULTS

A. The model

We consider an open one-dimensional lattice of L sites. An occupation number τ_i is associated with a site i , where $\tau_i = 0$, if site i is empty and $\tau_i = 1$, if site i is occupied. The dynamics of the model follows the discrete time backward-sequential rules [16, 17]. During each discrete moment of time t , an update of the configuration of the whole chain with L sites, labelled by $i = 1, 2, \dots, L$, takes place in $L + 1$ steps, passing through successive updates of the right boundary site $i = L$, all the pairs of nearest-neighbor sites in the backward order $(L - 1, L), \dots, (i, i + 1), \dots, (1, 2)$, and, finally, the left boundary site $i = 1$ is updated. According to the generalized backward-sequential rules:

1. Each integer time moment t (configuration update) starts with the update of the last site of the chain: if site $i = L$ is occupied, the particle at it is removed from the system with probability β and stays in place with probability $1 - \beta$. If the last particle has left the system, then the particle at site $i = L - 1$ takes its place at site $i = L$ with modified probability p_m ; otherwise, it remains immobile with probability $1 - p_m$.

2. Next, a particle at site $i = 1, 2, \dots, L - 2$ hops to an empty site $i + 1$ with probability p or p_m , depending on the update of the next nearest neighbor on the right-hand side at the current moment of time. If site i is occupied and site $i + 1$ is empty at the beginning of the current update, then the particle from site i jumps to site $i + 1$ with probability p and stays immobile with probability $1 - p$. Alternatively, if site $i + 1$ is occupied at the beginning of the current moment of time t , and became empty after the particle from $i + 1$ jumped to the empty $i + 2$, then the particle at site i jumps to site $i + 1$ with probability p_m and stays

immobile with probability $1 - p_m$.

3. The left boundary condition also depends on the occupation history of the right nearest-neighbor. If site $i = 1$ was empty at the beginning of the current update, a particle enters the system with probability α or site $i = 1$ remains empty with probability $1 - \alpha$. Alternatively, if site $i = 1$ was occupied at the beginning of the current moment of time, but became empty under its current update, then a particle enters the chain with probability $\tilde{\alpha}$ or the site remains empty with probability $1 - \tilde{\alpha}$, where

$$\tilde{\alpha} = \min\{1, \alpha p_m / p\}. \quad (1)$$

We note that the above left boundary condition was introduced first by Hrabák in [27] and, independently, in [24]. It is necessary for consistency with the special cases of backward-ordered sequential update, when $p_m = p$ and $\tilde{\alpha} = \alpha$, as well as with the parallel one, when $p_m = 0$ and $\tilde{\alpha} = 0$.

B. Known results in particular cases

Here we summarize the known results about the phase diagrams and the phase transitions between the stationary phases in the particular cases of $p_m = p$ (the ordinary backward-sequential update) and $p_m = 1$ (irreversible aggregation). The corresponding phase diagrams are shown in Fig. 1.

In Fig. 1(a) the subregions AI (BI) and AII (BII) differ by the shape of the local density profiles. The nonequilibrium phase transitions between low-density phase, LD=AIUAII, and maximum-current phase, MC, as well as between high-density phase, HD=BIUBII, and MC, are continuous, while the transition between LD and HD is discontinuous, with a finite jump in the local density. The exact critical injection/ejection rate values are $\alpha_c = \beta_c = 1 - \sqrt{1 - p}$. In our case of $p = 0.6$, $\alpha_c = \beta_c = 0.367544\dots$

In Fig. 1(b) the many-particle phase MP contains a macroscopic number of particles or clusters of size $O(1)$ as $L \rightarrow \infty$; MPI and MPII differ only by the shape of the local density profile, which results from the different type of evolution of the configuration gaps. In the region of MPI, the inequality $\beta > p$ leads to growing average width of the rightmost gap, hence the profile bends downward near the chain length. In the complementary region MPII, the opposite inequality $\beta < p$ holds and the rightmost gap is short-living, while the gaps

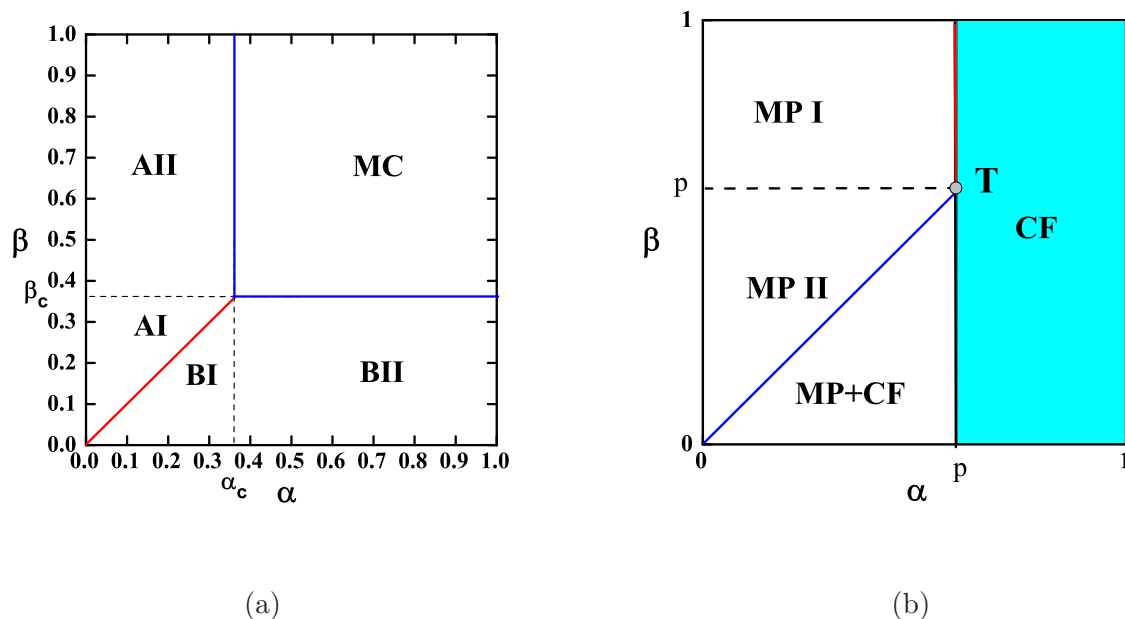


FIG. 1. (Color online) Phase diagrams in the $\{\alpha, \beta\}$ -plane of: (a) the standard TASEP with backward-sequential update with $p = p_m = 0.6$. There are three stationary phases: maximum-current phase, MC, low-density phase, LD=AI \cup AII, and high-density phase, HD=BI \cup BII; (b) the gTASEP with $p = 0.6$ and $p_m = 1$. The three stationary phases are of different nature: a many-particle phase MP=MP I \cup MP II, a CF phase of completely filled chains, and a mixed MP+CF phase.

on the left-hand side of it have a critical type of evolution with mean lifetime of the order $O(L^{1/2})$, see Ref. [26]. The phase MP+CF is mixed in the sense that the completely filled configurations are perturbed by short living gaps entering the chain from the first site. The configurations of the stationary nonequilibrium phase CF represent a completely filled chain with current $J = \beta$. The unusual phase transition, found in [24], takes place across the boundary $\alpha = p$ between the MP I and CF phases.

III. THE GENERIC CASE OF ATTRACTION

Firstly, we aim here to analytically approach the question of how the completely filled phase (CF) at $p_m = 1$ (see Fig. 1(b)) is destroyed, when $0 < 1 - p_m \ll 1$, and transformed into new phases typical for $p_m < 1$ (see Fig. 1(a)). One of the methods, developed in Refs.

[25, 26], and which is used also here, is based on the study of the time evolution of single gaps in different regions of the CF phase.

Secondly, we present results of extensive computer simulations, which suggest the topology of the modified phase diagram, the shift of the triple point $(\alpha_c(p, p_m), \beta_c(p, p_m))$ under the change of $p_m \in [p, 1]$ at fixed p , and the nature of the phase transitions between the stationary nonequilibrium phases.

A. Time evolution of configuration gaps

We begin with finding out the probability of a single gap appearance under boundary conditions corresponding to the CF phase. Then we consider the first step in the time evolution of the gap width. The problem is rather complicated because the probability of appearance of a gap is position dependent when $p_m < 1$. In contrast to the case of $p_m = 1$, here we show that when $\beta \neq p$, the gap width performs a special, position dependent random walk.

Let $P_i(p, p_m)$ denote the probability of appearance of a single gap at site $i = 1, 2, \dots, L$ in a completely filled configuration with $\tau_1 = \tau_2 = \dots \tau_L = 1$, when $0 < 1 - p_m \ll 1$. For brevity of notation, we do not show the explicit dependance on the injection and ejection rates of that probability. Since we exclude the appearance of a second gap, under the generalized backward-sequential update we obtain,

$$P_{L-k}(p, p_m) = (1 - p_m)p_m^k\beta, \quad k = 0, 1, \dots, L - 2, \quad P_1(p, p_m) = (1 - \tilde{\alpha})p_m^{L-1}\beta. \quad (2)$$

Under the assumption $0 < 1 - p_m \ll 1$, the left boundary condition yields $\tilde{\alpha} = 1$ for all $p < \alpha \leq 1$, which means that $P_1(p, p_m) = 0$ at the beginning of each update. Therefore, we focus on the case when the gap appears at sites $2 \leq i \leq L$. Then, the right edge of the gap, positioned at site $i + 1 < L$ can move one site to the right, provided that site is empty. The latter event occurs only if the particle at site $i = L$ leaves the system with probability β , and the remaining cluster of $L - i - 1$ particles at sites $i + 1, \dots, L - 1$ moves as a whole entity one site to the right, which happens with probability p_m^{L-i-1} . Thus, the total probability for the particle at the right edge to hop to the right is $p_m^{L-i-1}\beta$, and to remain at its place is $(1 - \beta) + (1 - p_m^{L-i-1})\beta$. On the other hand, the particle at the left edge $i - 1$, being either the rightmost particle of a cluster or isolated, may hop to the right with the position

independent probability p , and stay immobile with probability $1 - p$. As a result, the gap width increases by one site with probability

$$p_g(i) = (1 - p)p_m^{L-i-1}\beta, \quad (3)$$

decreases by one site with probability

$$q_g(i) = [(1 - \beta) + (1 - p_m^{L-i-1})\beta]p = (1 - p_m^{L-i-1}\beta)p, \quad (4)$$

and remains the same with probability

$$r_g(i) = 1 - p + p_m^{L-i-1}\beta(2p - 1). \quad (5)$$

As expected, at $p_m = 1$ these expressions reduce to equalities (4) in Ref. [26]. As is readily seen, in the alternative case of several coexisting gaps, the above probabilities apply exactly to the rightmost one.

Now we have to average the gap width evolution over the initial probabilities given by (2). The probability normalization factor under the condition of a single gap opened at sites $i = 2, 3, \dots, L$ is

$$N(p, p_m) = (1 - p_m)\beta \sum_{k=0}^{L-2} p_m^k = \beta(1 - p_m^{L-1}). \quad (6)$$

Then, the changes in the gap width at the first time step, averaged over all events of gap appearance at sites $i = 2, 3, \dots, L$, become as follows:

The gap width increases by one site with probability

$$\bar{p}_g = \frac{(1 - p)(1 - p_m)\beta}{p_m(1 - p_m^{L-1})} \sum_{k=2}^L p_m^{2k} = \frac{(1 - p)(1 + p_m^{L-1})\beta}{p_m(1 + p_m)}, \quad (7)$$

decreases by one site with probability

$$\bar{q}_g = \frac{p(1 - p_m)}{(1 - p_m^{L-1})} \sum_{k=0}^{L-2} (p_m^k - p_m^{2k-1}\beta) = p - \frac{p(1 + p_m^{L-1})\beta}{p_m(1 + p_m)}, \quad (8)$$

and remains the same with probability

$$\bar{r}_g = \frac{(1 - p_m)}{(1 - p_m^{L-1})} \sum_{k=0}^{L-2} [(1 - p)p_m^k + p_m^{2k-1}\beta(2p - 1)] = 1 - p + \frac{(2p - 1)\beta(1 + p_m^{L-1})}{p_m(1 + p_m)}. \quad (9)$$

Notably, at $p_m = 1$ the above results reduce again to equalities (4) in Ref. [26].

By comparing the expressions for \bar{p}_g and \bar{q}_g , we conclude that on the average a single-site gap will grow after the first time step of its evolution when

$$\beta > p \frac{p_m(1+p_m)}{(1+p_m^{L-1})}. \quad (10)$$

When $p_m \rightarrow 1$ and L is fixed, or $L \rightarrow \infty$ so that $p_m^L \rightarrow 1$, this condition simplifies to $\beta > p$. However, for fixed values of p_m close to 1, p_m^L will decrease to zero as $L \rightarrow \infty$. For example, in our computer simulations we used: $p_m = 0.99$ and $L = 800$, which yields $p_m^{L-1} \simeq 3.22 \times 10^{-4}$ and the criterion becomes much stronger, $\beta > 1.97p$. However, with each time step $j = 1, 2, \dots$ the right edge of the gap will hop forward by one site with increasing probability $p_m^{L-i-j}\beta$, while its left edge may hop to the right with the position independent probability p . Thus, the value of $p_g(i)$ will increase and the value of $q_g(i)$ will decrease in the course of time.

Without going into the involved details of the complete gaps evolution, we conjecture that the simple criteria $\beta > p$ for growing gaps, and $\beta < p$ for decreasing gaps, hold true. Thus, our expectation, confirmed by the computer simulations, is that in the upper region $(p < \alpha \leq 1] \times (p < \beta \leq 1]$ of the CF phase a maximum-current phase will appear. Its local density profile satisfies the inequalities $\rho_1 = 1 > \rho_{l/2} > \rho_L$, which follow from the conditions $\tilde{\alpha} = 1$, and the larger probability of gap formation near the end of the chain. In the lower region $(p < \alpha \leq 1] \times (0 < \beta < p]$ of the CF phase the gaps are scarce, small and short-living, which is indicative of a high-density phase. Again, the left-hand side of the local density profile bends upward to $\rho_1 = 1$.

Note that in the above consideration $p = \lim_{p_m \rightarrow 1-0} \sigma_c(p, p_m)$. In the case of $p_m < 1$, the critical values should decrease down to $\sigma_c(p, p) = 1 - \sqrt{1-p}$, as $p_m \rightarrow p + 0$.

B. Phase diagram and phase transitions

We performed Monte Carlo simulations of the gTASEP on open chains of mainly $L = 800$ and $L = 1600$ sites. Each run started with 10^6 relaxation updates and had not less than 10^4 attempted updates per lattice site. The stationary properties were evaluated by averaging over 100 (quasi)independent runs. The estimated accuracy is $O(10^{-3})$ for the local particle density and $O(10^{-4})$ for the current.

First, we compare the behavior of the current, J , and the local density at the midpoint

of the chain, $\rho_{1/2}$, under two modified hopping probabilities $p_m = 0.6$ and $p_m = 0.9$, as a function of the input rate α , at chain length $L = 800$ sites, fixed $p = 0.6$ and output rate $\beta = 0.8$, see Fig. 2.

We recall that in the standard backward-sequential TASEP with $p = 0.6$, the exact results in the thermodynamic limit $L \rightarrow \infty$ are: for the critical injection/ejection values

$$\alpha_c = \beta_c = 1 - \sqrt{1 - p} = 0.367544 \dots,$$

for the current in the maximum-current phase

$$J^{MC} = \frac{1 - \sqrt{1 - p}}{1 + \sqrt{1 - p}} = 0.225148 \dots,$$

and for the midpoint density in the MC phase

$$\rho_{1/2}^{MC} = \frac{1}{1 + \sqrt{1 - p}} = 0.612574 \dots$$

The critical value α_c , shown in Fig. 2 by a vertical green dashed line, corresponds to the transition of the asymptotic behavior of the current J (at $p_m = 0.6$) near α_c from a parabolic

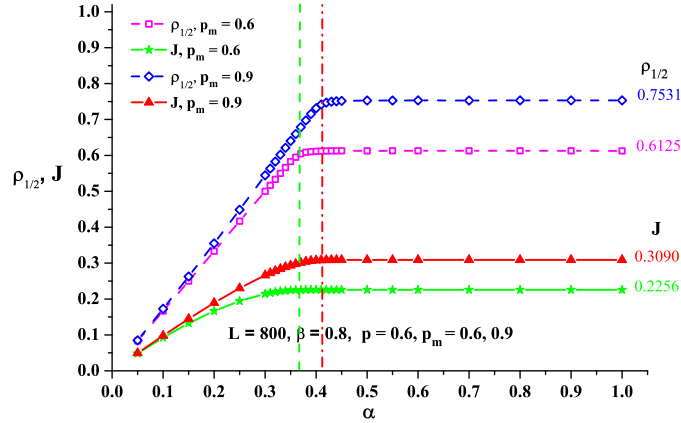


FIG. 2. (Color online) Behavior of the stationary midpoint density, $\rho_{1/2}$, and the current, J , for the gTASEP for two values of the modified hopping probability, $p_m = 0.6$ and $p_m = 0.9$, as a function of the input rate α at chain length $L = 800$ sites, fixed $p = 0.6$ and output rate $\beta = 0.8$. Apparently, their behavior (for $p_m = 0.6$ and for $p_m = 0.9$) is similar and reflects the continuous nonequilibrium phase transition across the segment $\beta_c(p, p_m) < \beta \leq 1$, however, with different, p_m -dependent critical values: our estimates for $p_m = 0.9$ are $\alpha_c(0.6, 0.9) = \beta_c(0.6, 0.9) \simeq 0.41$ (shown by the vertical red dashed-dotted line).

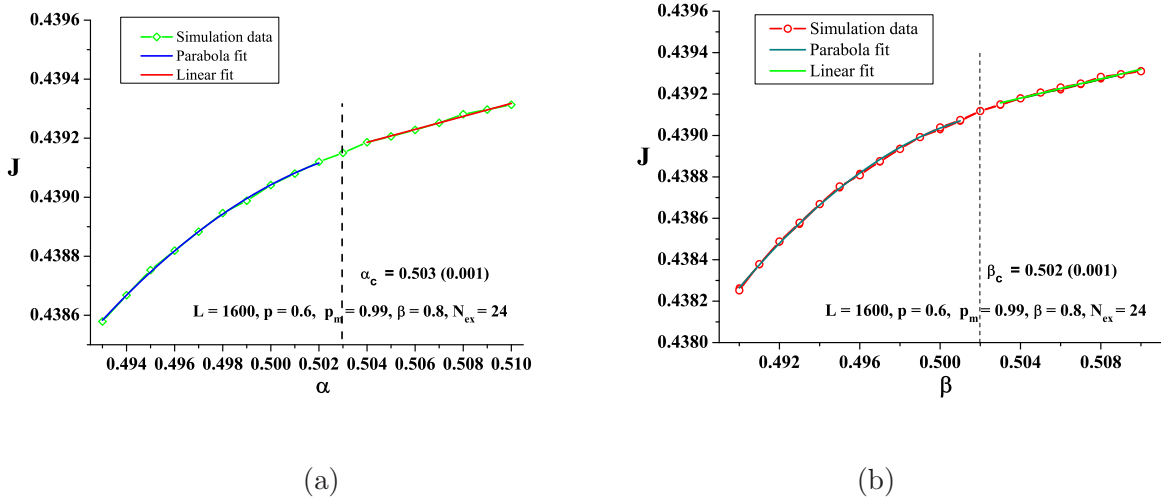


FIG. 3. (Color online) The current in the gTASEP when $p = 0.6$, $p_m = 0.99$ and $L = 1600$ sites, as a function of: (a) the injection probability α (at $\beta = 0.8$). The critical value $\alpha_c(0.6, 0.99) = 0.503 \pm 0.001$ is estimated from the apparent change in the asymptotic behavior of the current; (b) the ejection probability β (at $\alpha = 0.8$). The critical value $\beta_c(0.6, 0.99) = 0.502 \pm 0.001$ is estimated from the apparent change in the asymptotic behavior of the current.

one on the left-hand side of the segment $\beta_c(0.6, 0.6) < \beta \leq 1$, to a constant value in the MC phase on the right-hand side of it. Due to finite-size effects, the current J^{MC} slightly grows with α up to 0.2256 at $\alpha = 1$.

Similarly, at $p_m = 0.9$, we see that the phase transition across the segment $\beta_c(0.6, 0.9) < \beta \leq 1$ is continuous too and we estimate the critical values $\alpha_c(0.6, 0.9) = \beta_c(0.6, 0.9) \simeq 0.41$, see the vertical red dash-dotted line in Fig. 2. This indicates that the unusual phase transition, found in [24] at $p_m = 1$ across the boundary $\alpha = p$ becomes a continuous one. Note that in the MC phase the current grows up to $J^{MC}(0.6, 0.9) = 0.3090 \dots$ and the local density $\rho_{1/2}^{MC}(0.6, 0.9)$ up to 0.7531.

To check the continuity of the phase transition across the segment $\beta_c < \beta \leq 1$, we consider in more detail both the α - and β -dependance of the current on larger lattice and value of p_m closer to 1, namely $L = 1600$ and $p_m = 0.99$. The results are shown in Fig. 3(a) and (b).

It is instructive to analytically check the above estimates for the critical values of the injection (ejection) α_c (β_c) probabilities, commonly denoted by σ_c . To this end we use the continuity condition for the first derivative of the current: $J'(\sigma_c - 0) = J'(\sigma_c + 0)$. Close to

the critical value σ_c , we have a parabolic approximation for the current below σ_c ,

$$J(\sigma < \sigma_c) = A + B\sigma + C\sigma^2, \quad (11)$$

and a linear approximation above σ_c ,

$$J(\sigma > \sigma_c) = a + k\sigma. \quad (12)$$

Hence, in the case of a continuous second order phase transition, when $J'(\sigma_c-0) = J'(\sigma_c+0)$, we obtain an estimate for σ_c :

$$\sigma_c = \frac{k - B}{2C}. \quad (13)$$

In the case of the current as a function of α , see Fig. 3(a), the best least-square fit yields:

$$A = -0.386 \pm 0.05, \quad B = 3.229 \pm 0.21, \quad C = -3.186 \pm 0.21, \quad k = 0.022 \pm 7.7 \times 10^{-4}, \quad (14)$$

which leads to the estimate $\alpha_c = 0.503 \pm 0.07$. In spite of the large error interval, this estimate coincides with our former value of $\alpha_c(0.6, 0.99) \simeq 0.503$.

In the complementary case of the β -dependent current, see Fig. 3(b), the best least-square fit yields:

$$A = -0.536 \pm 0.055, \quad B = 3.86 \pm 0.22, \quad C = -3.82 \pm 0.22, \quad k = 0.023 \pm 0.001, \quad (15)$$

which leads to the estimate $\beta_c = 0.502 \pm 0.05$. Again, the error bars are rather large, but this estimated value also coincides with our former assessment of $\beta_c(0.6, 0.99) \simeq 0.502$. Finally, we assume that within error bars $\alpha_c(0.6, 0.99) = \beta_c(0.6, 0.99) = 0.502 \pm 0.02$.

Now we focus on the phase transitions taking place by changing α across the segment $0 < \beta < \beta_c(p, p_m)$. In Ref. [24], a mixed MP+CF phase was found at $p_m = 1$, see Fig. 1(b). This phase is characterized by the nonzero probability $P(1)$ of appearance of a cluster spanning the whole chain of L sites: $P(1)$ changes with α from zero at the left phase boundary $0 < \alpha = \beta < p$ to $P(1) = 1$ at the right boundary $\alpha = p$, $0 < \beta < p$ with the CF phase. In Ref. [26] the MP+CF phase was interpreted as a boundary perturbed one. Here we show that as $p_m < 1$, $P(1)$ exponentially decreases to zero, not only in the MP+CF phase but also in the subregion $(0 < \alpha < \alpha_c) \times (0 < \beta < \beta_c)$, which at $p_m = 1$ belongs to the CF phase. The results of our computer simulations for the cluster-size distribution in gTASEP when $p_m = 0.99$ at $\alpha = 0.6$, $\beta = 0.25$, and lattice sizes $L = 200, 400, 800$ are shown in Fig. 4.

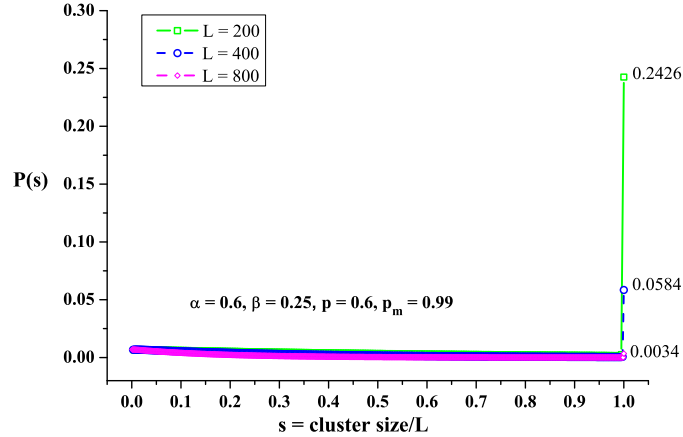


FIG. 4. (Color online) Cluster size distribution in the gTASEP when $p = 0.6$, $p_m = 0.99$ on lattices $L = 200, 400, 800$ sites at $\alpha = 0.6$, and $\beta = 0.25$. At $L = 1600$ the estimated value of $P(1)$ drops down to 1.147×10^{-5} .

By using a larger series of chain sizes, from $L = 200$ to $L = 1600$, we obtain that $P(1)$ probability decays exponentially fast with the unlimited increase of L ,

$$P_L(1) \simeq 0.2426 \times \exp\{-(L - 200)/140\}, \quad L \geq 200. \quad (16)$$

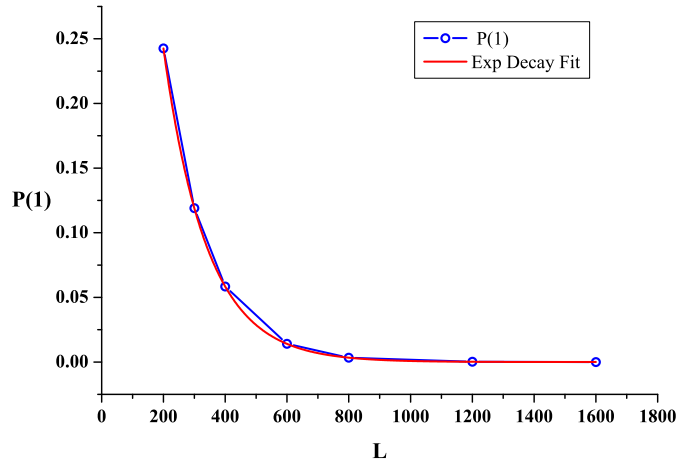


FIG. 5. (Color online) Least-square fit to the exponential decay of the complete-cluster probability $P(1)$ with the unlimited increase of the chain length L in the gTASEP when $p = 0.6$ and $p_m = 0.99$ at $\alpha = 0.6$ and $\beta = 0.25$.

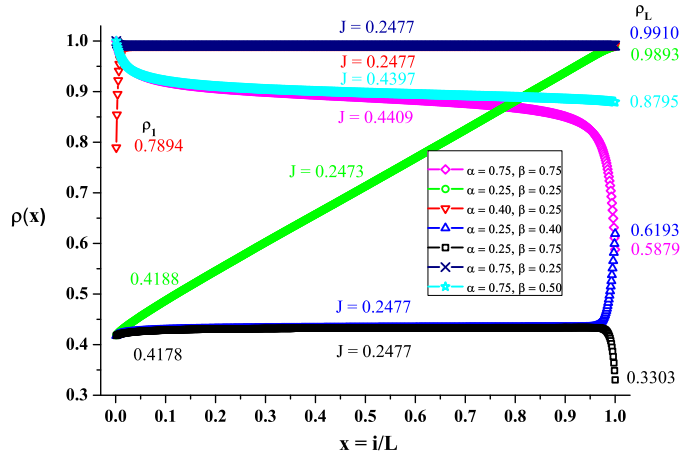


FIG. 6. (Color online) Local density profiles of the gTASEP when $p = 0.6$ and $p_m = 0.99$ at different points in the phase space. Obviously, the point $(\alpha = 0.25, \beta = 0.25)$ lies on the coexistence line between the low-density phase, represented by the points $(\alpha = 0.25, \beta = 0.40)$ and $(\alpha = 0.25, \beta = 0.75)$, and the high-density phase, represented by the points $(\alpha = 0.40, \beta = 0.25)$, $(\alpha = 0.75, \beta = 0.25)$ and $(\alpha = 0.75, \beta = 0.50)$. The corresponding value of the current J is denoted next to every density profile.

The quality of the fit is illustrated in Fig. 5.

Therefore, by continuity arguments, we conclude that in the thermodynamic limit $L \rightarrow \infty$ the regions between the left-hand boundary $0 < \alpha = \beta < \sigma_c(p, p_m)$ and the right-hand boundary at $\alpha = 1$ and $0 < \beta < \beta_c(p, p_m)$, belong to the same phase. The fact that across the coexistence line $0 < \alpha = \beta < \sigma_c(p, p_m)$ there occurs a first-order phase transition is seen from the shape of the local density profiles, shown in Fig. 6 at different points (α, β) in the $\alpha - \beta$ plane.

By using continuity arguments, we generalize the above results to conjecture a generic phase diagram of the gTASEP with $p_m < 1$ with the same topology as in the case of the backward-sequential TASEP, see Fig. 1(a), but with (p, p_m) -dependent triple point (α_c, β_c) . In Fig. 7 we exemplify the phase diagram of the gTASEP in the particular case of $p = 0.6$ and $p_m = 0.99$ and the shift of the triple point (α_c, β_c) with the increase of p_m at fixed $p = 0.6$.

Now one can see the similarity in the behavior of the local density profiles in the cases

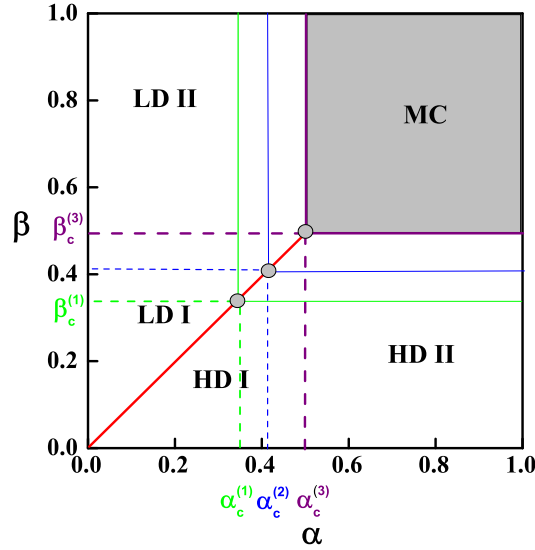


FIG. 7. (Color online) Conjectured phase diagram of the gTASEP when $p = 0.6$ and $p_m = 0.99$ (purple lines). It has the same topology as in the case of the standard TASEP with backward-sequential update (shown in Fig. 1(a)), but with different, p_m -dependent critical values – our estimates are $\alpha_c^{(3)}(0.6; 0.99) = \beta_c^{(3)}(0.6; 0.99) = 0.502$, see text. To illustrate the shift of the triple point we have added also the critical lines corresponding of the TASEP with backward sequential update, i.e., $\alpha_c^{(1)}(0.6; 0.6) = \beta_c^{(1)}(0.6; 0.6) = 0.3675$ (thin green lines), and also of the gTASEP when $p = 0.6$ and $p_m = 0.9$ – $\alpha_c^{(2)}(0.6; 0.9) = \beta_c^{(2)}(0.6; 0.9) = 0.41$ (thin blue lines).

$p_m = p < 1$ and $p < p_m < 1$. In the low-density phase LD = LDIULDII the bulk density is less than $1/2$, the difference between the LDI and LDII regions is in the right-hand end of the local density profile: in LDI it bends upward, while in LDII it bends downward, similarly to the case of the standard backward-sequential TASEP. This can be readily explained by using the exact relationship $\rho_L = J/\beta$, and assuming the same value of the current in the two regions. In the considered particular case of $p = 0.6$ and $p_m = 0.99$, the bulk density in the high-density phase is very close to 1, the difference between the regions HDI and HDII being at left-hand side of the profile: in HDI it sharply bends downward, while in HDII it bends upward, again similarly to the case of the standard backward-sequential TASEP.

Additional information can be found in the different gaps evolution regimes in regions LDI and HDI: in both cases $\alpha < p$, which implies $\tilde{\alpha} < 1$, so that gaps can appear at the first

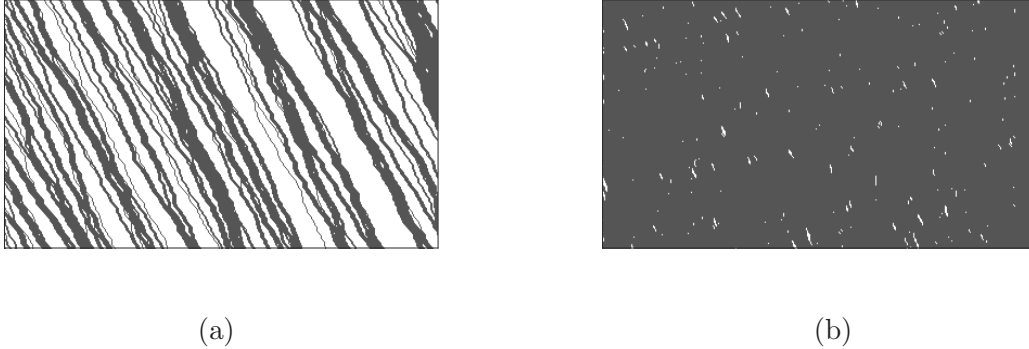


FIG. 8. A space-time plot (time is flowing downward in the vertical direction) of the gTASEP when $p = 0.6$, $p_m = 0.99$, and $L = 400$ sites, showing the gaps evolution, in: (a) region LDI ($\alpha = 0.25, \beta = 0.40$) – white stripes; (b) in region HDI ($\alpha = 0.40, \beta = 0.25$) – white spots.

site $i = 1$ and evolve throughout the chain; however, in LDI the gaps are wide and long-living, while in HDI they are small, scarce and very short living, compare Figs. 8(a) and 8(b). The typical gaps pattern in LDII (HDII) is similar to the one shown for LDI (HDI). These features may explain the large difference in the particle densities in the low-density and high-density phases.

Here we emphasize that the gTASEP does not satisfy the particle-hole symmetry inherent to the standard versions of TASEP. For example, the fundamental diagram of the generic model, obtained by Hrabák, see Fig. 6.2 in [27], where $\gamma = p_m/p$, is not symmetric under the replacement $\rho \leftrightarrow 1 - \rho$. The above mentioned phase diagram was obtained in the thermodynamic limit under periodic boundary conditions, which means that the very bulk dynamics at $p < p_m$ does not respect the particle-hole symmetry. In addition, in our case of open boundaries, the left boundary condition Eq. (1) is not appropriate for introduction of holes from the right chain end. Therefore, it is rather unexpected that the currents in the phases LD and HD, calculated at symmetric points (α, β) and (β, α) , are equal: $J^{LD}(\alpha = 0.25, \beta = 0.75) = J^{HD}(\alpha = 0.75, \beta = 0.25) \simeq 0.2477$.

IV. DISCUSSION

We studied the generalized TASEP in the regime of particle attraction ($p_m > p$) between hopping nearest-neighboring particles. In this case ($p < p_m < 1$) cluster aggregation and fragmentation is allowed in the system. A central problem of interest was to find how the

topology of the phase diagram in the case of irreversible aggregation $p_m = 1$, see Fig. 1(b), transforms into the topology of the well-known phase diagram of the usual TASEP with backward-ordered sequential update, see Fig. 1(a), when p_m decreases from $p_m = 1$ down to $p_m = p$. Based on an incomplete random-walk theory and on extensive Monte Carlo calculations, we conjectured that the above phenomenon takes place sharply, as soon as p_m becomes less than 1. The main difference between the phase diagrams for $p_m = 1$ and $p_m < 1$ turned out to be the dependence of the critical probabilities $\sigma_c(p, p_m)$ on p_m , at fixed p . Apart of that, we have shown the similarity of the local density profiles and the current as a function of the injection α and ejection β probabilities, in the cases $p_m = p$ and $p_m > p$. The main effect of increasing the modified hopping probability p_m turns out to be increase in the values of critical point coordinates, the bulk density and the current. For example, on passing from $p_m = p$ to $p_m = 0.99$, these values grow from

$$\alpha_c = \beta_c \simeq 0.3675, \quad J^{\text{MC}} \simeq 0.2251, \quad \rho_{1/2}^{\text{MC}} \simeq 0.6126,$$

to

$$\alpha_c = \beta_c \simeq 0.502, \quad J^{\text{MC}} \simeq 0.4409, \quad \rho_{1/2}^{\text{MC}} \simeq 0.8891.$$

On the ground of our random walk theory and the computer simulations, we have conjectured that the simple criteria $\beta > p$, for growing gaps, and $\beta < p$, for decreasing gaps, hold true on the average.

An interesting result is the exponential decay to zero of the probability $P(1)$ of a complete cluster in the HDII phase (which emerges in the lower region of the CF phase of the gTASEP with $p_m = 1$), when $p_m < 1$ and the chain length L increases unboundedly, see Fig. 5.

There are still many open problems, such as an elaboration of the random walk theory to the extend of yielding both qualitative and quantitative predictions, the analytical derivation of the local density at the chain ends and the value of the current in the different stationary phases, just to mention some.

ACKNOWLEDGMENTS

The authors gratefully acknowledge the fruitful discussions with their late colleague and coauthor Professor V.B. Priezhev, held at an early stage of the present study. NCP also

acknowledges the provided access to the e-infrastructure of the Centre for Advanced Computing and Data Processing, with the financial support by the Grant No BG05M2OP001-1.001-0003, financed by the Science and Education for Smart Growth Operational Program (2014-2020) and co-financed by the European Union through the European structural and Investment funds.

-
- [1] C. T. MacDonald, J. H. Gibbs, and A. C. Pipkin, *Biopolymers* **6**, 1 (1968).
 - [2] F. Zhang, C. L. Liu, and B. R. Hu, *J. Neurochemistry* **4**, 102 (2006).
 - [3] T. Tipathi and D. Chowdhury, *Phys. Rev. E* **77**, 011921 (2008).
 - [4] P. Guelich, A. Garai, K. Nashinari, A. Schadschneider, and D. Chowdhury, *Phys. Rev. E* **75**, 041905 (2007).
 - [5] A. B. Kolomeisky, *Phys. Rev. Lett.* **98**, 048105 (2007).
 - [6] A. Zilman, J. Pearson, and G. Bel, *Phys. Rev. Lett.* **103**, 128103 (2009).
 - [7] K. Nagle, *Phys. Rev. E* **53**, 4655 (1996).
 - [8] D. Chowdhury, L. Santen, and A. Schadschneider, *Phys. Rep.* **329**, 199 (2000).
 - [9] C. Arita, M. E. Foulaadvand, and L. Santen, *Phys. Rev. E* **95**, 032108 (2017).
 - [10] D. Helbing, *Rev. Mod. Phys.* **73**, 1067 (2001).
 - [11] B. Derrida, E. Domany, and D. Mukamel, *J. Stat. Phys.* **69**, 667 (1992).
 - [12] G. M. Schütz and E. Domany, *J. Stat. Phys.* **72**, 277 (1993).
 - [13] B. Derrida, M. R. Evans, V. Hakim, and V. Pasquier, *J. Phys. A* **26**, 1493 (1993).
 - [14] H. Hinrichsen, *J. Phys. A* **29**, 3659 (1996).
 - [15] A. Honecker and I. Peschel, *J. Stat. Phys.* **88**, 319 (1997).
 - [16] N. Rajewski, A. Schadschneider, and M. Schreckenberg, *J. Phys. A* **29**, L305 (1996).
 - [17] N. Rajewski and M. Schreckenberg, *Physica A* **139**, 245 (1997).
 - [18] M. R. Evans, N. Rajewsky, and E. R. Speer, *J. Stat. Phys.* **95**, 45 (1998).
 - [19] J. de Gier and B. Nienhuis, *Phys. Rev. E* **59**, 4899 (1999).
 - [20] M. Wölki, *Steady States of Discrete Mass Transport Models (Master thesis)* (University of Duisburg-Essen, 2005).
 - [21] A. E. Derbyshev, S. S. Poghosyan, A. M. Povolotsky, and V. B. Priezhev, *J. Stat. Mech.* **2012**, P05014 (2012).

- [22] A. E. Derbyshev, A. M. Povolotsky, and V. B. Priezzhev, *Phys. Rev. E* **91**, 022125 (2015).
- [23] B. L. Aneva and J. G. Brankov, *Phys. Rev. E* **94**, 022138 (2016).
- [24] N. Z. Bunzarova and N. C. Pesheva, *Phys. Rev. E* **95**, 052105 (2017).
- [25] N. Z. Bunzarova, N. C. Pesheva, V. Priezzhev, and J. G. Brankov, *J. Phys: Conf. Series* **936**, 012026 (2017).
- [26] J. G. Brankov, N. Z. Bunzarova, N. C. Pesheva, and V. Priezzhev, *Physica A* **494**, 340 (2018).
- [27] P. Hrabák, *Ph.D. Thesis* (Czech Technical University, Faculty of Nuclear Sciences and Physical Engineering, Praga, 2014).